Acta Chemica Scandinavica, 1997: 51: 8–12
Printed in UK – all rights reserved

ACTA
CHEMICA SCANDINAVICA
ISSN 0904-213X

Structure and Phase Relations in the $NdCl_3$–NdOCl System

Heidi Mediaas,[a] George Photiadis,[b] George N. Papatheodorou,[b] Jens E. Vindstad[a] and Terje Østvold*,[a]

[a]Institute of Inorganic Chemistry, Norwegian University of Science and Technology, N-7034 Trondheim, Norway and [b]The Institute of Chemical Engineering and High Temperature Chemical Processes, FORTH, PO Box 1414, 26500 Patras, Greece

Mediaas, H., Photiadis, G., Papatheodorou, G. N., Vindstad, J. E. and Østvold, T., 1997. Structure and Phase Relations in the $NdCl_3$–NdOCl System. – Acta Chem. Scand. 51: 8–12. © Acta Chemica Scandinavica 1997.

Raman spectra of liquid mixtures of the $NdCl_3$–NdOCl binary confirm that the network-like structure of chlorine edge-sharing $NdCl_6^{3-}$ octahedra in pure liquid $NdCl_3$ is not changed significantly by the addition of NdOCl. Freezing-point depression data at the $NdCl_3$ (l/s) phase boundary confirm this conclusion, and suggest that O^{2-} ions are built into this structure as $Nd_nOCl_{3n+2}^{4-}$ anions with $n \geq 2$.

The published phase diagram of the $NdCl_3$–Nd_2O_3(NdOCl) system is not in agreement with the present data, showing smaller Nd_2O_3(NdOCl) solubilities together with higher melting points at the $NdCl_3$(l/s) boundary than the published data.

Neodymium metal is an essential component for the manufacturing of powerful Nd–Fe–B permanent magnets.[1] The metal is being produced from $NdCl_3$ dissolved in a molten alkali chloride–calcium chloride salt bath by metallothermic or electrolytic reduction.[2] An understanding of such mixtures will therefore be important in elucidating and maybe improving the abovementioned production processes. The $NdCl_3$–AlkCl (Alk = Na, K, Rb and Cs) phase diagrams are well established.[3,4] These mixtures have also been studied by high-temperature calorimetry,[5] and Raman spectra have been reported showing mainly octahedral $NdCl_6^{3-}$ species.[6] It is well known that oxide species of neodymium will dissolve readily in liquid $NdCl_3$.[7] A phase diagram is reported showing an eutectic point of 722 °C at 93 mol% $NdCl_3$–7 mol% Nd_2O_3, corresponding to 80.4 mol% $NdCl_3$–19.6 mol% NdOCl, which forms when Nd_2O_3 dissolves in liquid $NdCl_3$.[7]

We have reinvestigated the $NdCl_3$–NdOCl system to try to establish the structure of melt species in this binary, and at the same time we have redetermined the $NdCl_3$ and NdOCl liquidus lines, since the published phase diagram[7] seems to be somewhat in error because of a melting point of $NdCl_3$ that is too low.[8–10]

Experimental

The chemicals used were $NdCl_3 \cdot 6H_2O$ (p.a. Heraeus 99.9%), Nd_2O_3 (p.a. Heraeus 99.9%), HCl (Messer Griesheim 99.8%), N_2 (Norsk Hydro 99.99%) and Ar (Norsk Hydro 99.998%). Anhydrous $NdCl_3$was made by slowly heating the hexahydrate first under N_2 and then under an HCl atmosphere up to 580 °C over 100 h. This salt still contained 0.2 wt% O^{2-} as determined by carbothermal reduction analysis using a Leco TC-436 apparatus. By further vacuum distillation of this salt at 1000 °C and 10^{-5} mbar, we obtained a good quality $NdCl_3$ with a very low O^{2-} content (0.002 wt%) and with a melting point of 759.3 ± 0.1 °C. This is in very good agreement with the accepted fusion temperature of pure $NdCl_3$.[8–10] NdOCl was produced by mixing $NdCl_3$ with Nd_2O_3, which was vacuum dried at 350 °C, keeping $NdCl_3$ in excess. This mixture was melted at 830 °C and kept for 2 h in a gold crucible under dry Ar in a glove box with less than 1 ppm H_2O. This ensured complete conversion of Nd_2O_3 to NdOCl. After the reaction between $NdCl_3$ and Nd_2O_3 was completed, the salt batch was cooled to room temperature, and the salt was washed in distilled water to remove excess $NdCl_3$. NdOCl was filtered, washed and dried at 140 °C for 24 h and subsequently heated to 900 °C for 1 h. The final product showed the X-ray pattern of NdOCl,[11,12] and contained 8.18 ± 0.05 wt% O^{2-} according to Leco TC-436 analysis, which compares well with a theoretical value of 8.18 wt%.

Leco TC-436. Oxide analysis, which is a carbothermal reduction of oxide to CO(g) and a subsequent catalytic conversion of CO to CO_2(g) detected by IR, was used

* To whom correspondence should be addressed.

to determine the oxide content of the starting materials and melt samples. The liquidus line at the NdOCl(s) phase boundary was determined by oxide analysis of melt samples taken at given temperatures with NdOCl(s) present in excess. The Leco method to determine oxide contents of hydroscopic salts has been described in previous papers.[13,14]

Raman spectroscopy. Owing to the corrosive nature of the $NdCl_3$–NdOCl liquid mixtures these could not be contained in silica cells, and a Raman cell of the windowless type made of graphite contained in a silica envelope was used.[15] The salt mixtures to be used in the Raman cell were premelted in a small graphite crucible under an inert atmosphere and kept for several hours to ensure dissolution of NdOCl. This salt mixture was quenched to ensure homogeneity, and an appropriate amount was transferred to the Raman cell such that the optical 'windows' of the cell were filled with the liquid mixture. The Raman apparatus and the optical furnace used have been described elsewhere.[16] The Raman spectra of the present samples were obtained using the 488 nm line of the Ar^+ laser. Liquids were recorded using the two different polarization planes of the incident light to the scattering plane; HV (horizontal) and VV (vertical).

Liquidus lines. The $NdCl_3$ liquidus was measured by cryoscopy in an argon filled glove box with a water content < 1 ppm and an oxygen content < 5 ppm. The furnace with the gold crucible contained in a silica cell positioned in a Kanthal tube tightly connected to the glove box is shown in Fig. 1. The cryoscopic studies were performed with 50–80 g salt in the crucible, and the temperature was measured with a calibrated Pt,Pt10%Rh thermocouple using a differential voltmeter equipped with a strip-chart recorder.

The molten salt mixtures were stirred and equilibrated at about 30 °C above the melting point for times sufficient to dissolve the added oxide before liquidus temperatures were measured. The cooling rate was from 1 to 3 °C/min. Small crystals of $NdCl_3$ (<0.005 g) were added at the expected freezing-point temperature to prevent supercooling. The difference between successive measurements at the same melt composition gave SD = 0.5 °C. The composition of the melt was changed by additions of Nd_2O_3 pellets through a charging tube positioned just above the melt surface. Samples of the melt were withdrawn using a silica tube containing a silica filter (pore size 15–40 μm) at the bottom. This sampling tube was immersed in the melt only during sampling.

The NdOCl liquidus was determined by equilibrating $NdCl_3$(l) with NdOCl(s) in excess in three separate experiments at given temperatures in the range $740 < T/°C < 840$. Melt samples were then analysed for O^{2-} by the Leco technique. The necessary equilibration time for the reaction

$$NdOCl(s) = NdOCl\ [\text{dissolved in } NdCl_3(l)] \qquad (1)$$

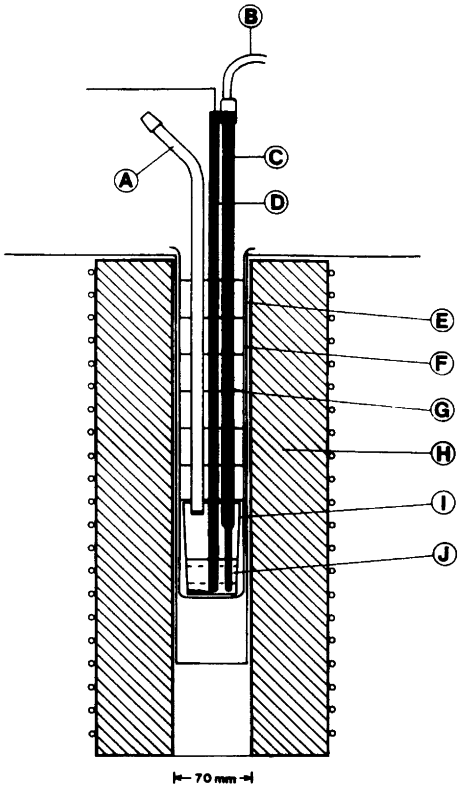

Fig. 1. Cell for equilibrium studies. (A) Silica sampling tube with a silica sinter porosity 3 at the tip; (B) flexible wire connected to stirring motor; (C) stirrer, alumina rod with Au casing at the tip; (D) thermocouple Pt/Pt10%Rh in alumina tubing with Au casing at the tip; (E) Kanthal tube tightly connected to glove box; (F) silica cell; (G) alumina radiation shields; (H) furnace; (I) Au crucible; (J) melt.

was established in a separate experiment. We have measured the concentration of NdOCl in $NdCl_3$(l) as a function of time at 805 °C with NdOCl(s) in excess. The equilibration time seems to be around 10 h. Some experiments were also performed with NdOCl(s) additions, giving smaller concentrations than saturation. By a gradual increase in the NdOCl concentration, saturation was reached. In Fig. 2 data from such an experiment at 783 °C are presented, showing that the ratio NdOCl (analysed)/NdOCl (added) = 1.

Result and discussion

Raman spectra. Figure 3 presents the Raman spectra of pure liquid $NdCl_3$ and of two molten NdOCl–$NdCl_3$ mixtures. Careful examination of the high-frequency range of the NdOCl–$NdCl_3$spectra up to 1200 cm^{-1} showed no bands due to neodymium oxygen vibrations. Raman spectra in the frequency range up to 500 cm^{-1} of pure molten $NdCl_3$ have been reported previously.[6] Its structure is dominated by distorted $NdCl_6^{3-}$ octahedra sharing edges through chloride ions, similar to that suggested for molten YCl_3.[17] Raman-active modes ($A_{1g}+E_g+F_{2g}$) of ideal (O_h) octahedra were

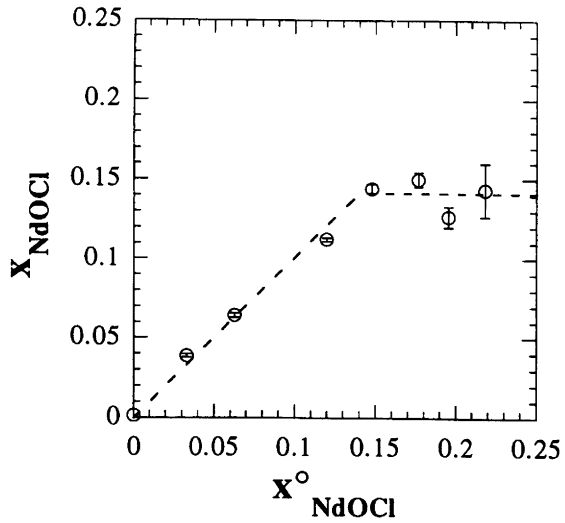

Fig. 2. NdOCl analysed vs. NdOCl added in $NdCl_3$–NdOCl melt samples at 783 °C. SD: I.

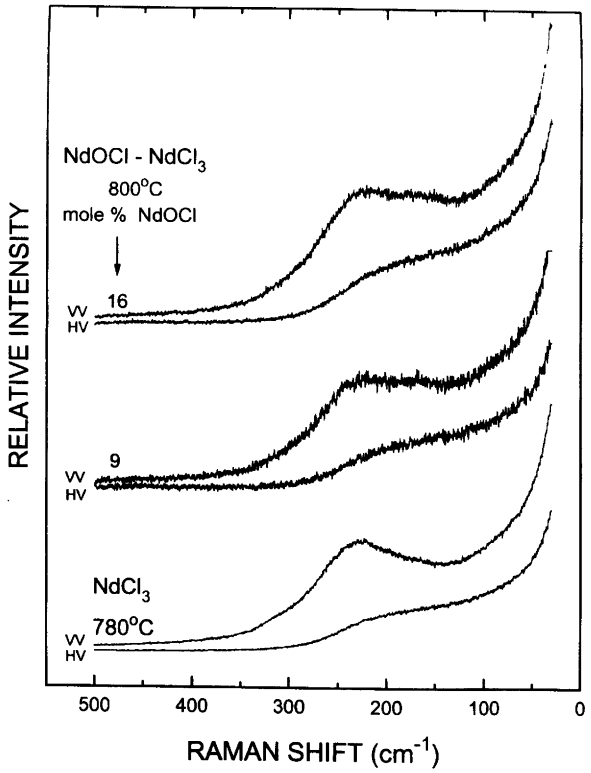

Fig. 3. Raman spectra of $NdCl_3$ and NdOCl–$NdCl_3$ melts, $\lambda_0 =$ 488 nm, power 150 mW, slits 3 cm^{-1}, time constant 0.3 s, scan rate 2 cm^{-1} s^{-1}.

correlated with distorted D_3 symmetry octahedra present in molten $NdCl_3$, according to the proposed scheme[17]

$$A_{1g} \rightarrow A_1, \quad E_g \rightarrow E, \quad F_{2g} \rightarrow A_1 + E$$

Use of Raman spectra in the reduced form revealed the following bands:[6] $\nu(A_1) = 251\ cm^{-1}$, $\nu(E) = 225\ cm^{-1}$, $\nu(A_1) = 320\ cm^{-1}$ and $\nu(E) = 125\ cm^{-1}$.

A comparison between the Raman spectrum of pure liquid $NdCl_3$ with spectra of molten NdOCl–$NdCl_3$ mixtures shows that the latter, in addition to bands attributed to $NdCl_3$, exhibit a polarized band at ca. 175 cm^{-1}. Spectral features of the molten mixtures indicate that the network-like structure of chlorine edge-sharing $NdCl_6^{3-}$ octahedra in liquid $NdCl_3$[6] is not changed significantly by the addition of NdOCl.

Solid NdOCl has the tetragonal PbFCl-type structure belonging to the space group D_{4h}^7 (*P4/nmm*). The structure consists of $(NdO)_n^{n+}$ layers of edge-sharing ONd_4tetrahedra, alternating with sheets of Cl^- anions.[12] Vibrational spectra (IR or Raman) of NdOCl powder are reported.[18,19] Assignments of the Raman active modes of NdOCl were given, assisted by normal coordinate analysis. Owing to some minor discrepancies in these studies, the assignments given are not strictly correct. Single-crystal Raman spectra based on polarization measurements[20] probably assigned the observed frequencies correctly as: $\nu(E_9) = 118\ cm^{-1}$, $\nu(A_{1g}) = 183\ cm^{-1}$, $\nu(E_g) = 219\ cm^{-1}$, $\nu(A_1, B_{2g}) = 352\ cm^{-1}$ and $\nu(E_g) = 465\ cm^{-1}$. The polarized band clearly seen at ca. 175 cm^{-1} for our NdOCl–$NdCl_3$ melts in Fig. 3 is close to the polarized band (A_{1g}) at 183 cm^{-1} observed for solid NdOCl. This band probably involves a translational motion of a Cl site coupled to the translational motion of an Nd site in the solid structure.[19]

In the spectra of pure $NdCl_3$ liquid the broad band of ca. 250 cm^{-1} is predominantly due to a distribution of Nd–Cl stretching vibrations of distorted octahedra bridged by edges through monovalent chlorines to neighbouring distorted octahedra.[6] The addition of NdOCl in the melt introduces the divalent oxygen, which presumably is surrounded by neodymium atoms forming bridging bonds with them. The substitution of one or two bridging chlorines of the octahedra with an oxygen diminishes the bonding of neodymium with the remaining chlorines, and thus shifts the Nd–Cl frequency to the 'red'. This is more likely the reason for the observed Nd–Cl frequency shift on going from the pure $NdCl_3$ ($\nu \approx 250\ cm^{-1}$) into the oxygen-containing melt ($\nu \approx 175\ cm^{-1}$). Furthermore all the neodymium atoms bonded or bridged through oxygen have weaker chlorine bridging bonds to the rest of the network-like melt, creating a cluster-like entity which involves two or more neodymium atoms. A general formula for such a species would be $[Nd_nOCl_{n+m}]$ ($n \geq 2$), with n and m being unknown. Our cryoscopic data (see following section) indicate the formation of such units in the melt.

The Raman spectra of $NdCl_3$–KCl and NdOCl–$NdCl_3$–KCl melts are presented in Fig. 4. The binary $NdCl_3$–KCl ($x_{NdCl_3} > 0.25$) is also reported to contain distorted $NdCl_6^{3-}$ edge-sharing octahedra.[6] This distortion is not as pronounced as in pure $NdCl_3$, however. An additional weak polarized band is observed at 175 cm^{-1} in the NdOCl–$NdCl_3$–KCl mixtures. This indicates the same structural modification of the $NdCl_3$–KCl binary as of the pure $NdCl_3$ where NdOCl is added.

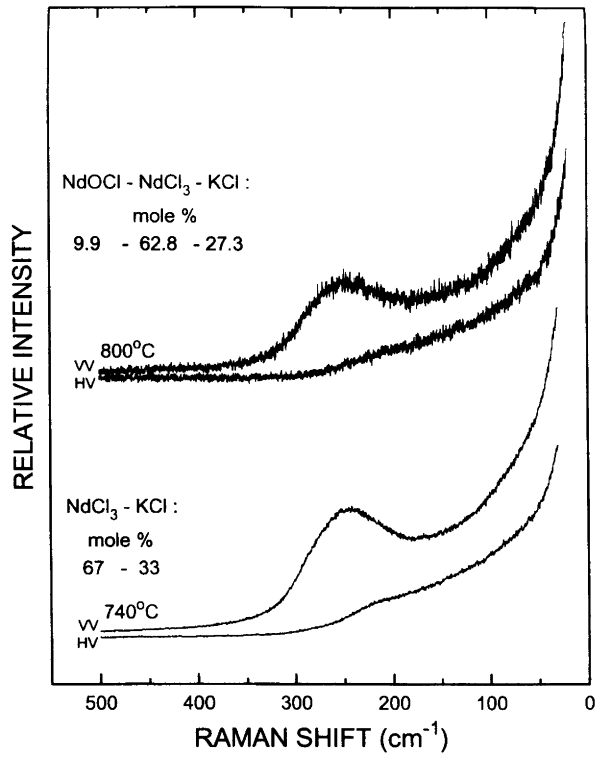

Fig. 4. Raman spectra of $NdCl_3$–KCl and NdOCl–$NdCl_3$–KCl melts. Spectral conditions as in Fig. 3.

The liquidus line. for the $NdCl_3$(s/l) boundary is determined by cryoscopy. Data are given in Fig. 5 and in Table 1. At this boundary the major difference between the present and published data[7] is the higher liquidus temperatures reported in the present work. This may be reasonable in view of the efforts made by us to obtain oxide-free $NdCl_3$ and high-quality NdOCl. We also tried to determine the $NdCl_3$ liquidus line by measuring the NdOCl concentration at the $NdCl_3$(l/s) phase boundary. Sampling was, however, difficult, owing to the solid

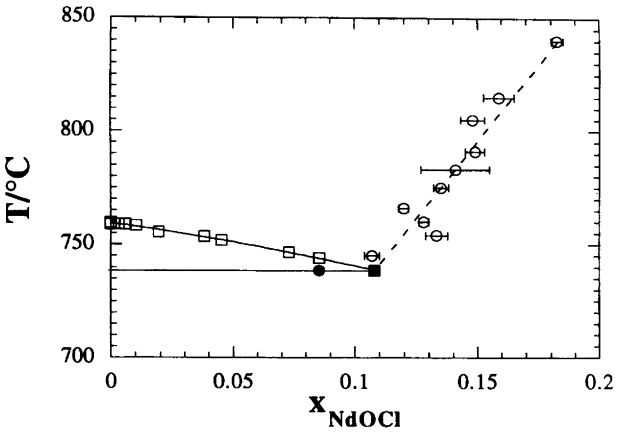

Fig. 5. Measured liquidus lines for the $NdCl_3$–NdOCl binary. An average value of x_{NdOCl} is given at 783 °C (see also note in Table 2). Ref. Fig. 2. □, Cryoscopy; ○, Leco oxide analysis of solidified liquid samples; |——|, SD: ●, solidus temperature; ■, estimated eutectic point.

Table 1. Crystallization temperatures as obtained by cryoscopy for the $NdCl_3$ rich side of the $NdCl_3$–NdOCl system.

	T/°C, SD	
Mol% NdOCL	Liquidus	Solidus
0	759[a]	
0	759.3, 0.1	
0.331	759.0, 0.1	
0.586	758.9, 0.2	
1.03	758.4, 0.2	
1.94	755.5, 0.1	
3.81	753.5, 0.2	
4.50	751.9, 0.3	
7.30	746.6, 0.1	
8.54	744.2, 0.2	738.6, 0.3
10.8[b]	738.6	

[a] Ref 8. [b] Estimated eutectic point composition.

$NdCl_3$formed. In Table 2 and Fig. 5 data for the NdOCl(s/l) liquidus line are also reported. The oxide solubilities are much smaller than reported previously.[7] Our oxide analysis given in Fig. 2 seems to be reasonably accurate, and the new version of the phase diagram for the $NdCl_3$–NdOCl binary given in Fig. 5 is probably more accurate than the diagram published previously.[7]

In Fig. 6 the freezing-point depression data are plotted vs. x_{NdOCl} and compared with model calculations using the cryoscopic equation

$$T - T_{fus} = \Delta T \approx R \ln a_{NdCl_3} T_{fus}^2 / \Delta_{fus} H_{NdCl_3} \quad (2)$$

In the calculations $T_{fus} = 759.3\,°C$ and $\Delta_{fus} H_{NdCl_3} = 50.2\,kJ\ mol^{-1}$ [10] are used, together with $a_{NdCl_3} = x_{Nd^{3+}} x_{Cl^-}{}^3 \gamma_{NdCl_3}$, where γ_{NdCl_3} is considered to be constant for small additions of NdOCl. As can be seen

Table 2. Oxide concentration in $NdCl_3$–NdOCl melts at different temperatures. Oxide contents were obtained from solidified melt samples by the Leco technique.

	Mol% NdOCl			
T/°C	Weighed in	Measured	SD	Comments
745		10.7	0.3	NdOCl (s) present
754		13.3	0.4	NdOCl (s) present
760		12.8	0.2	NdOCl (s) present
766		12.0	0.2	NdOCl (s) present
775		13.5	0.3	NdOCl (s) present
783	3.30	3.89	0.1	
783	6.28	6.43	0.1	
783	12.0	11.2	0.1	
783	14.25	14.4	0.3	NdOCl (s) present
783	17.69	14.99	0.5	NdOCl (s) present
783	19.54	12.7	0.7	NdOCl (s) present
783	21.83	14.3	1.7[a]	NdOCl (s) present
791		14.9	0.4	NdOCl (s) present
805		14.8	0.05	NdOCl (s) present
815		15.9	0.6	NdOCl (s) present
840		18.2	0.2	NdOCl (s) present

[a] The melt sample was not quenched due to experimental problems. This caused inhomogeneity. 18 parallels (the whole sample) were analysed giving a large SD.

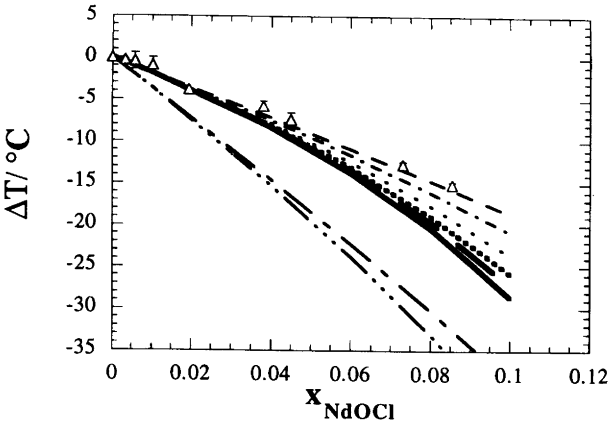

Fig. 6. Measured, △, and calculated $NdCl_3$ liquidus lines: (—) NdO^+ or NdOCl; (-·-·-) $Nd_2OCl_3^+$ or Nd_2OCl_4; (...) Nd_3OCl^{6+} or Nd_3OCl_7; (-··-) $NdCl_2^+$ and $NdOCl_2^-$; (-····) $NdCl_2^+$ or $Nd_2OCl_5^-$; ·····: $Nd_2OCl_8^{4-}$; ——: $Nd_3OCl_{11}^{4-}$; ————: $Nd_4OCl_{14}^{4-}$.

from Fig. 6, only one new species is formed when NdOCl dissolves in $NdCl_3$. Three possible reactions may explain this observation.

The first explanation involves the formation of a new cation NdO^+ or $Nd_nOCl_{3(n-1)}^+$ with $n \geqslant 2$, the second the formation of a new neutral species, Nd_nOCl_{3n-2}, and the third the formation of an anion of the type $Nd_nOCl_{3n+2}^{4-}$.

All three explanations will fit the observed freezing point depression data at low NdOCl additions, as can be observed from Fig. 6. A neutral component is, however, less reasonable in view of the ionic character of the present melt system. The formation of one new anion and one new cation is obviously not possible owing to freezing point depressions for such models that are too large, as shown by Fig. 6. The Raman data, however, indicate the formation of Nd_nOCl_{n+m} species with an excess of chlorine atoms bonded to the neodymium. A negative charge is anticipated, thus the only new species proposed that fulfil this requirement are the $Nd_nOCl_{3n+2}^{4-}$ type anions with $n \geqslant 2$. Such anions can also explain the solubility of NdOCl, since the molar ratio Nd/O is between 5 and 3 at saturation. It is, of course, possible to suggest other octahedral anion species which will fulfil the requirements set both by the experimental Raman spectra and the cryoscopic data. It is, however, a rather limited number of possible anionic species which have a reasonable negative charge. This in our opinion is an important restriction on the model ions, since highly charged ions will only be stable in melts dilute in $NdCl_3$, and when $NdCl_3$ is mixed with the heavy alkali chlorides.

Concluding remarks

Raman spectra confirm that the structure of $NdCl_3$–NdOCl melts contains distorted $NdCl_6^{3-}$ octahedra sharing edges through chloride ions. Together with freezing-point depression and NdOCl solubility data, the Raman spectra indicate that the O^{2-} ions are built into this structure as $Nd_nOCl_{3n+2}^{4-}$ species with $\geqslant 2$. The present data also confirm that the phase diagram of the $NdCl_3$–Nd_2O_3(NdOCl) system should be revised.

Acknowledgements. This work has been supported by the Human Capital and Mobility Program of The European Communities and The Research Council of Norway. Some of the experimental data were obtained by the Siv.ing. students Baard Kaasa and Trond Berg.

References

1. Croat, J. J., Herbst, J. F., Lee, R. W. and Pinkerton, F. E. *J. Appl. Phys. 55* (1984) 2078.
2. Sharma, R. A. *J. Met. 39* (1987) 33.
3. Sharma, R. A. and Rogers, R. A. *J. Am. Ceram. Soc. 75* (1992) 2484.
4. Seifert, H. F., Fink, H. and Uebach J. *Therm. Anal. 33* (1988) 625.
5. Gaune-Escard, M., Bogacz, A., Rycerz, L. and Szczepaniak, W. *Mater. Sci. Forum 73–75* (1991) 61.
6. Photiadis, G., Voyiatzis, G. A. and Papatheodorou, G. N. *Molten Salt Forum 1–2* (1993/94) 183.
7. T'en, F. N., and Morozov, I. S. *Russ. J. Inorg. Chem. 14* (1969) 1179.
8. Dworkin, A. S. and Bredig, M. A. *J. Phys. Chem. 67* (1963) 697.
9. Druding, L. F. and Corbett, J. D. *J. Am. Chem. Soc. 83* (1991) 2462.
10. Barin, I. *Thermochemical Data of Pure Substances*, VCH, Weinheim 1989.
11. Zachariassen, W. H. *Acta Crystallogr. 2* (1949) 389.
12. Aride, J., Chaminade, J. P. and Pouchard, M. *J. Cryst. Growth 57* (1982) 194.
13. Mediaas, H., Vindstad, J. E. and Østvold, T. *Light Metals*. W. Hale, Warrendale, PA 1996.
14. Kipouros, G., Mediaas, H., Tkatcheva, O., Vindstad, J. E. and Østvold, T. *Light Metals*. W. Hale, Warrendale, PA 1996.
15. Gilbert, B., and Materne, T. *Appl. Spectrosc. 44* (1990) 299.
16. Boghosian, S. and Papatheodorou, G. N. *J. Phys. Chem. 93* (1989) 415.
17. Papatheodorou, G. N. *J. Chem. Phys. 66* (1977) 2893.
18. Basile, L. J., Ferraro, J. R. and Cronet, D. *J. Inorg. Nucl. Chem. 33* (1971) 1047.
19. Hase, Y., Dusstan, L. and Temperini, M. L. A. *Spectrochim. Acta, Part A 37* (1981) 597.
20. Del Cul, G. D., Nave, S. E., Begun, G. M. and Peterson, J. R. *J. Raman Spectrosc. 23* (1992) 267.

Received January 4, 1996.